SLIDING SHEAR IN CRACKED REINFORCED CONCRETE SHEAR WALLS SUBJECTED TO REVERSED CYCLIC SHEAR

Hiroshi Noguchi (I)
Masao Ochiai (II)
Shinichi Ihzuka (III)
Presenting Author: Hiroshi Noguchi

SUMMARY

The shear failure test results of twenty-four reinforced concrete shear wall specimens were reported. The specimens were grouped into the three series. In A series, the shear plane was subjected to uniform normal stress. In B series, the shear plane was subjected to bending moment and compressive axial force. In C series, the longitudinal reinforcement ratio and uniform compressive normal stress on the shear plane were selected as the experimental parameters. The process to failure, the failure mode, the shear strength and the contributions of internal shear transfer (IST) and dowel action of longitudinal reinforcement were discussed.

INTRODUCTION

There are frequent occasions when shear forces are transferred across existing cracks initiated by the shrinkage, thermal stress or seismic bending moment and shear force. Umemura et al. reported that the sliding shear failure occurred along flexural cracks or lateral reinforcement near the boundary to the base of box-type shear wall specimens in the laboratory tests. (Ref. 1) The sliding shear failure was observed also in the actual earthquake damage. In Skopje a 5 to 8 cm displacement occurred at a wall. The box structure of the Nethercutt Museum displaced about 10 mm at a construction joint in the wall of 200 mm thickness during the San Fernando earthquake. (Ref. 2)

Previous studies on the sliding shear failure were carried out by Mattock (Ref. 3), Gergely (Refs. 2 and 4), Paulay (Ref. 5) and Aoyagi (Ref. 6) by the direct shear testing method. In this study, the model specimens of shear walls were manufactured simulating real structures as far as possible. Shear tests were carried out for the following three series: (A) with uniform normal stress on the shear plane, (B) with strain gradient on the shear plane, and (C) with two experimental parameters, longitudinal reinforcement ratio and uniform compressive normal stress on the shear plane.

(I)   Associate Professor, Department of Architectural Engineering, Chiba University, Chiba, Japan

(II) Structural Division, Tokyo Office of Daiken Architects and Engineering Company, Tokyo, Japan

(III) Postgraduate, Department of Architectural Engineering, Chiba University, Chiba, Japan

SHEAR TRANSFER TEST SERIES A AND B

Specimens

In A and B series, the shear transfer strength across a crack and the contributions of shear transfer components were mainly studied. Four specimens in A series were subjected to uniform normal stress on the shear plane, and four specimens in B series were subjected to strain gradient on the shear plane. The detail of B series specimens was shown in Fig. 1. The gross longitudinal reinforcement ratio across the shear plane was $p_s = 1.0\%$. The detail of A series specimens was the same as B series except that the lateral reinforcement ratio was $p_s' = 1.0\%$, and there was no bent-up shear reinforcement.

The shear failure plane was set at the center of the specimen by introducing notches of 20 cm depth from both sides of the specimens as shown in Fig. 1. A crack was pre-formed by pure-tension on the shear plane of each specimen except for A4. The variables among specimens were shown in Table 1. For specimen, A3, longitudinal reinforcing bars across the shear plane were covered by flexible vinyl sleeves in order to eliminate the dowel action of longitudinal reinforcement, and only the effect of interface shear transfer (IST) across the crack was studied. For A4, the crack width was made 0.1 mm, and the crack surface was made smooth using a thin greased copper plate at the shear plane in order to eliminate shear transfer across the crack.

In B series specimens, bending moment and axial compressive force was applied to produce the strain gradient on the shear plane. The value of bending moment was chosen such that the strain gradient should be produced as shown in Table 1 at the calculated ultimate shear strength. For specimens, B1 and B2, the strain of the overall section was in compression. For B3 and B4, there were both tensile and compressive strains along the shear plane.

The material properties of concrete and reinforcement were shown in Table 2.

Testing Method

Loading arrangement was shown in Fig. 2. (Ref. 7) A couple of forces for controlling the axial force and bending moment on the shear plane was applied by four 35tf hydraulic jacks. The reversed cyclic lateral shear force was applied one cycle each at 50%, 70%, 90% and 100% of the ultimate shear strength calculated from Birkeland's equation (Ref. 8) provided that the deflections of specimens, A3, A4 and B2 were equal to A1, A1, and B1, respectively.

Process to Failure

The ultimate crack patterns for specimens A1 and B1 were shown in Fig. 3. At failure in A series specimens longitudinal reinforcement across the shear plane yielded immediately, and followed by slip along the shear plane. In B series specimens, the yielding of longitudinal reinforcement across the shear plane was not observed except for specimen B4. At failure the extensive compression spalling of concrete occurred in the zone surrounded by small inclined cracks initiated at the fourth loading cycle, as shown in Fig. 3.

Load-slip relations along the shear plane were shown in Fig. 4. For
A1, the shape of loops showed the contrary S-type for the second and the sub-
sequent cycles. For A2, at the maximum load of the fourth cycle the slip
immediately took place and hereafter the load-slip curve showed the contrary
S-type. For the dowel specimen A4, the residual slip for each cycle came
to be nearly zero. In B series, the hysteresis loops were spindle-shaped
for all specimens. It may be explained by the following two reasons. The
compressive axial force was relatively large, and the effect of the inclined
crack opening near the tip of a notch on the measuring position of the slip
was significant, which was different from A series.

Strains in Longitudinal Reinforcement

In A series specimens, most of reinforcing bars yielded near the ultimate
strength, as shown in Fig. 5. In B series specimens, the yielding of rein-
forcement was not observed in B1 - B3 even near the ultimate strength except
for B4. Therefore, when a compressive axial stress was a level of 60 kgf/cm^2,
the ultimate shear strength seemed to be dependent upon the compressive
failure of concrete.

Ultimate Shear Strength

Birkeland's original equation (Ref. 8) for the ultimate shear strength
was modified as follows for B series specimens. The concrete stress, σ_0 and
reinforcement stress, σ_s (tension in positive) were calculated for each rein-
forcement across the shear plane with Umemura's e-function method assuming
that the plane section remained plane. It could be assumed that at the
ultimate strength the reinforcement yielded and the additional compressive
stress term $\rho_v f_y$ was replaced with $\rho_v (f_y - \sigma_s)$. Therefore,

$$_B V_u = 8.87 \sqrt{\rho_v (f_y - \sigma_s)} + \sigma_0 \quad (kgf/cm^2) \tag{1}$$

where $\rho_v = A_{vf}/A_{cr}$ (A_{vf}: cross sectional area of reinforcement, A_{cr}: cross
sectional area of the shear plane), f_y was the yielding strength of rein-
forcement.

According to Mattock (Ref. 9), when the ultimate shear strength was
decided by the yielding of reinforcement, the strength was represented by
Eq.(2). When the strength was decided by the compressive failure of concrete,
the strength was represented by Eq.(3).

$$_M V_u = 0.8\{\rho_v (f_y - \sigma_s) + \sigma_0\} + 28.12 \quad (kgf/cm^2)$$
$$\text{but } \rho_v (f_y - \sigma_s) + \sigma_0 \leqslant 90. \tag{2}$$
$$_M V_u = 0.143\{\rho_v (f_y - \sigma_s) + \sigma_0\} + 80 \quad (kgf/cm^2)$$
$$\text{but } \rho_v (f_y - \sigma_s) + \sigma_0 > 90. \tag{3}$$

As the linear approximation of Aoyagi's test data, the following equation
was adopted. (Ref. 6)

$$_A V_u = \sqrt{f_c'} \left[2.6 + 0.105 \times 0.5 \times \{\rho_v (_e\sigma_s - \sigma_s) + \sigma_0\} \right] \quad (kgf/cm^2)$$
$$\text{and less than } 6.5\sqrt{f_c'} \tag{4}$$

where $_e\sigma_s$ was the stress of reinforcement measured just before the shear
failure.

In Table 3, the comparisons between the ultimate shear strength calculated from Eq.(1) - Eq.(4) and test results were shown. Fig. 6 showed the relations between the ultimate shear strength calculated from Birkeland's equation (1) and bending moment. Test results for specimens B1 and B3 showed a good agreement with the calculated results. It could be pointed out from Eq.(1) that the effect of bending moment on the ultimate shear strength was fairly small, and this point corresponded to Mattock's qualitative test results. (Ref. 10) The ultimate shear strength and the failure mode for specimens B1 and B3 calculated from Mattock's equations (2) and (3) gave a good agreement with the test results as shown in Table 3. In case of B4, the calculated strength was decided by Mattock's equation (2) with the yielding of all reinforcement, but gave a conservative estimate. The calculated strength from Aoyagi's equation (4) gave a higher estimate for B1 and a lower estimate for B3 as shown in Table 3. It was difficult to obtain the strain in reinforcement correctly just before the failure load, and the upper limit, $_AV_u = 6.5\sqrt{f_c'}$ seemed to be uncertain because of lack of test data.

Contributions of IST and Dowel Action

The shear transfer mechanism of specimens A3 and A4 was IST and dowel action respectively. The hysteresis loops of A3 + A4, which were obtained from the superposition of load-slip curves of A3 and A4 at the same slip considering the hysteresis characteristics, gave a fairly good agreement with A1, as shown in Fig. 7. From Fig. 4 the contribution ratios of IST and dowel action were as follows, IST: 75 - 83%, dowel action: 17 - 25%. From the similar comparison of B1 with B2 (IST only) subjected to compressive axial stress ($\sigma_0 = 60 kgf/cm^2$), IST was 86 - 88%, and dowel action was 12 - 14%. In previous studies, IST and dowel action were 68 - 77% and 23 - 32% respectively, by Mattock (Ref. 10), and 75 - 80% and 15 - 25% by White (Ref. 4). Therefore, the test results gave a good agreement with those of Mattock and White under tensile axial stress.

SHEAR TRANSFER TEST SERIES C

Specimens

In C series, the effect of the reinforcement ratio and uniform compressive normal stress on the failure mode was mainly studied. Sixteen specimens were grouped into two sub-series, CA and CB, composed of eight specimens each. The variables among specimens were shown in Table 4. The reinforcement ratio varied from 0.8% to 2.0% and the uniform compressive normal stresses were zero and $20 kgf/cm^2$. The detail of specimens for CA sub-series was the same as A series except for the existence of a bent-up shear reinforcement, and the detail for CB sub-series was almost the same as B series. In this series, a crack was not pre-formed on the shear plane. The compressive strength of concrete, f_c' was 300 - 342 kgf/cm^2 and the yielding strength of the reinforcement, σ_6 was 3780 kgf/cm^2.

Testing Method

Loading arrangement in CB sub-series was shown in Fig. 8. While the lateral force was subjected from the one side of the loading beam in CA sub-series, the uniformly distributed shear force was subjected in CB sub-series. The reversed cyclic lateral shear force was applied one cycle each at 50%,

70%, 90% and 100% of the ultimate shear strength calculated from Yamada's equation as shown in Fig. 9. (Ref. 11)

Progress to Failure

The ultimate crack patterns were similar to ones for A and B series. For specimens, CA 1 - 6, the shear-compression failure preceded the sliding shear failure near the shear plane. But almost all reinforcing bars across the shear plane yielded near the ultimate strength. Therefore, it could be considered that the difference between the strength in the test and the sliding shear failure strength was small. For the other specimens, the process to failure was almost similar to A series.

Ultimate Shear Strength

The test results of the ultimate shear strength, τ_{max} were shown in Table 5, and the relations between $\tau_{max}/\sqrt{f_c'}$ and $p_{ws}\sigma_y$ were shown in Fig. 9. The yielding of all reinforcing bars across the shear plane was observed for specimens, CA 1 ~ 5, CB 1 ~ 3 and CB 5 ~ 6. It was considered that the strength of these specimens was due to the yielding of reinforcing bars across the shear plane. Meanwhile, the yielding of all reinforcing bars across the shear plane was not observed for CA 6 ~ 8, CB 4 and CB 7, 8. For these specimens, the strength seemed to be decided by the compressive failure of concrete.

For specimens, CA 7 ~ 8, CB 3 ~ 4 and CB 7 ~ 8, the strength reached the upper limit. From these test results, it was considered that the critical reinforcement ratio, $_{cr}p_w$ of specimens of which failure mode changed from the yielding of reinforcement to the compression failure of concrete were 1.6%, 1.6%, more than 1.2%, and 1.4% for CA (σ_0 = 0), CB (σ_0 = 0), CA (σ_0 = 20kgf /cm^2), and CB (σ_0 = 20kgf/cm^2) respectively. From Fig. 9, it was also shown that the critical reinforcement ratio got smaller when the compressive normal stress on the shear plane incresed. It seemed to be due to the differnce in the loading method that the strength in CA sub-series was a little higher than in CB sub-series.

The ultimate shear strength calculated from Birkeland's original equation (σ_s = 0 in Eq.(1)), and Mattock's, Aoyagi's and Yamada's equations was plotted in Fig. 9. Compared with test results, the shear strength for both cases, σ_0 = 0 and σ_0 = 20kgf/cm^2 in CA and CB sub-series was underestimated by Birkeland's equation. The increase of strength under axial compressive stress, σ_0 = 20kgf/cm^2 was overestimated. The upper limit of strength and the critical reinforcement ratio could not represented. The strength was overestimated by Mattock's equation in case of σ_0 = 0 in CA sub-series except for the upper limit. The increase of strength under axial compressive stress was also overestimated. But the reinforcement ratio gave a good agreement with test results. The shear strength calculated by Aoyagi's and Yamada's equations showed a similar tendency to the strength calculated by Mattock's equation. From these comparisons, it was pointed out that the ultimate shear strength could not be predicted well by the previous equations. This tendency was more remarkable under the axial compressive stress. This seems to be due to the existence of cracks across the shear plane in the wall. It was considered that there was still room for the further study in predicting the shear transfer strength of shear walls without a pre-formed crack.

CONCLUSIONS

The shear strength on the shear plane of shear walls with a pre-formed crack subjected to bending moment and axial force could be estimated by modifying previous equations. The effect of bending moment on the ultimate shear strength was fairly small. The shear strength under large compressive axial force seemed to be dependent upon the compressive failure of concrete. The shear strength of shear walls without a pre-formed crack was overestimated by almost previous equations. This seemed to be due to the existence of shear cracks across the shear plane.

ACKNOWLEDGEMENTS

REFERENCES

1) Umemura's Laboratory, "Experimental Study on the Strength and Restoring Force Chracterics of Reinforced Concrete Shear Walls," Research Report, Faculty of Engineering, University of Tokyo, Sept. 1975, pps.150.

2) Gergely, P, "Experimental and Analytical Investigation of Reinforced Concrete Frames Subjected to Earthquake Loading," Workshop on ERCBC, University of California, Berkeley, July 1977, pp.1175-1195.

3) Mattock, A.H., "The Shear Transfer Behavior of Cracked Monolithic Concrete Subjected to Cyclically Reversing Shear," Report SM 74-4, Univ. of Washington, Nov. 1974.

4) White, R.N., Gergely, P. and Jimenez, R., "Sliding Shear and Dowel Forces in Cracked Reinforced Concrete Subjected to Seismic Loading," AICAP-CEB Symp., Rome, May 1979, pp.77-84.

5) Paulay, T. and Loeber, P.J., "Shear Transfer by Aggregate Interlock," ACI SP-42, 1974, pp.1-15.

6) Aoyagi, Y. and Yamada, K., "On the Shear Transfer Mechanics of Reinforced Concrete," Proc. of Annual Conv., No.35, JSCE, Oct. 1978.

7) Aoyama, H. and Hosokawa, Y., "Experimental Study on the Behavior of Reinforced Concrete Shear Walls under Cyclic Loading (Part 5)," Annual Report, Engineering Research Institute, Univ. of Tokyo, Vol.38, 1979, pp.61-66.

8) Shaikh, A.F., "Proposed Revision to Shear-Friction Provisions," PCI Journal March-April 1978, pp.12-21.

9) Mattock, A.H., Hofbeck, J.A. and Ibrahim, I.O., "Shear Transfer in Reinforced Concrete," ACI Journal, Feb. 1969, pp.119-128.

10) Mattock, A.H., "Effect of Moment and Tension across the Shear Plane on Single Direction Shear Transfer Strength in Monolithic Concrete," Report SM 74-3, Univ. of Washington, Oct. 1974.

11) Yamada, K., "A Study on the Design of RC Containment for Nuclear Power Stations with Particular Reference to Rationaligation of RC Shell Elements against Shear Forces," Special Report of the Technical Research Institute of Maeda Construction Co. Ltd., No.22-1, March 1982, pps.106.
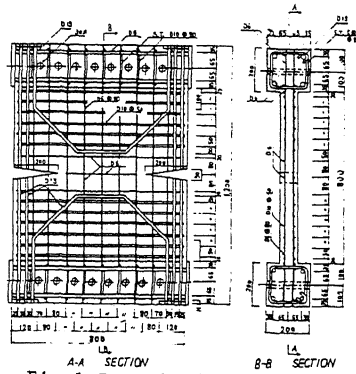
Fig.1 Detail of Specimens,
Unit(mm)

A-A SECTION   B-B SECTION

Table 1 Specimens

	Specimen	Axial Stress $\epsilon_x(T_f/cm^2)$	Shear Resistant Elements	Bending Moment (tonf·cm)	Strain Distribution
A Series	A1	+10	IST+Dowel	0	
	A2	−10	IST+Dowel	0	
	A3	+10	IST	0	
	A4	+10	Dowel	0	
B Series	B1	−60	IST+Dowel	Q x 4.88	
	B2	−60	IST	Q x 4.88	
	B3	−60	IST+Dowel	Q x14.2	
	B4	−20	IST+Dowel	Q x 4.97	

Table 2. Properties of Materials

Series		Normal Concrete					
		$cE_{1/4}$ (kgf/cm²)	F_c (kgf/cm²)	$c\epsilon_b$ (%)	σ_{sp} (kgf/cm²)	Slump (cm)	Age (days)
A		1.9x10⁵	161.9	0.20	19.5	15	57
B		2.49x10⁵	266.4	0.23	24.5	15.6	38

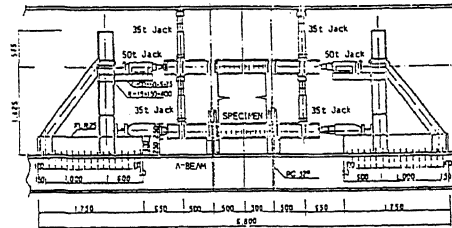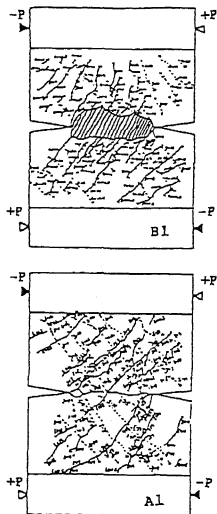|		Reinforcement				
		Area (cm²)	$s\sigma_y$ (kgf/cm²)	$s\sigma_{max}$ (kgf/cm²)	E_s (kgf/cm²)	$s\epsilon_{max}$ (%)
A	D-13	1.27	3389	5168	1.88x10⁶	19.5
	D- 6	0.32	3953	5155	1.75x10⁶	10.0
B	D-13	1.27	3381	4984	1.66x10⁶	20.3
	D-10	0.71	3732	5389	1.93x10⁶	16.7
	D- 6	0.32	3706	4944	1.69x10⁶	10.4

Fig.2 Loading Arrangement
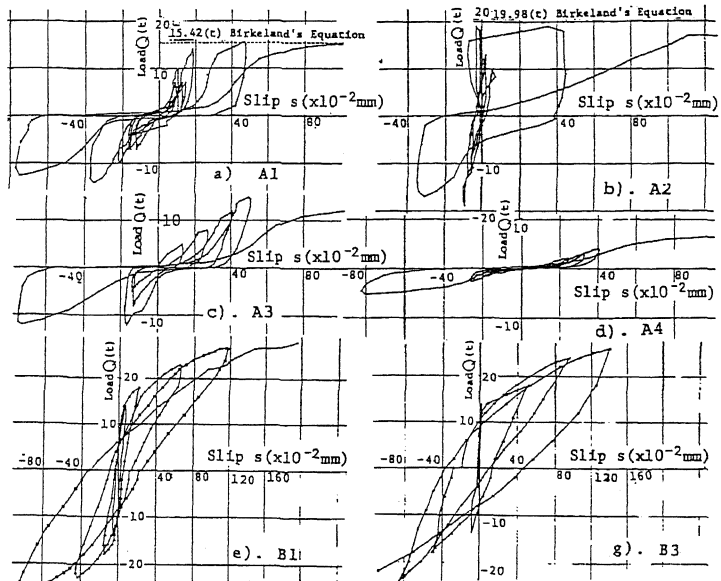

Fig.3 Ultimate Crack Patterns

Fig.4 Relations between Load and Slip along the Shear Plane

337
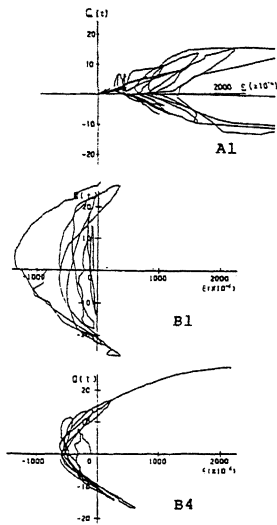
Fig.5 Load-Strain in
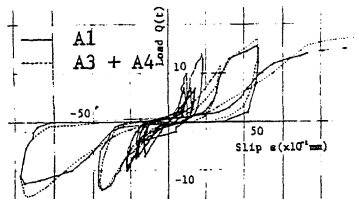Longitudinal Reinforcement
Relations

Fig.7 Comparisons of Load-Slip
between A1 and A3 + A4

Table.4　Specimens

		P_t (%)	$\sigma_o\left(\frac{kg}{cm^2}\right)$	Fc$\left(\frac{kg}{cm^2}\right)$			P_t (%)	$\sigma_o\left(\frac{kg}{cm^2}\right)$	Fc$\left(\frac{kg}{cm^2}\right)$
	CA 1	0.8	0	342		CB 1	1.2	0	300
CA	CA 2	0.8	20	342	CB	CB 2	1.4	0	300
S	CA 3	1.0	0	342	S	CB 3	1.6	0	300
E R	CA 4	1.0	20	342	E R	CB 4	1.8	0	300
I E	CA 5	1.2	0	340	I E	CB 5	1.0	20	310
S	CA 6	1.2	20	340	S	CB 6	1.2	20	310
	CA 7	1.6	0	340		CB 7	1.4	20	310
	CA 8	2.0	0	340		CB 8	1.6	20	310

Fig.8　Loading　Arrangement

Table 3. Comparisons of the Calculated
Shear Strength with Test Results

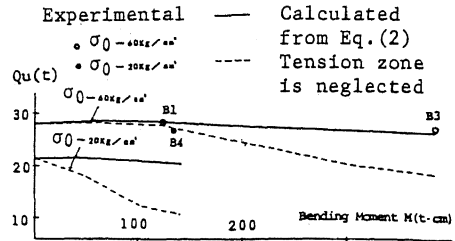|	Ultimate Shear Strength Q_u(tonf) (Ultimate Shear Stress v_u(kgf/cm^2))			
	Experiment	Birkeland Eq.(2)	Mattock Eq.(3),(4)	Aoyagi Eq.(5)
A1	15.8 (49.2)	15.4 (48.2)	16.5 (51.7)	16.9 (52.8)
A2	19.0 (59.4)	20.0 (62.4)	21.7 (67.7)	21.2 (66.2)
B1	27.9 (87.2)	28.1 (87.8)	29.0 (90.6)	29.8 (93.1)
B3	27.0 (84.4)	26.1 (81.6)	26.4 (82.5)	24.6* (76.9)*
B4	26.9 (84.1)	20.5 (64.1)	21.5 (67.2)	25.7 (80.3)

Fig.6 Relations between Ultimate
Shear Strength and Bending Moment

Table.5　Test Results

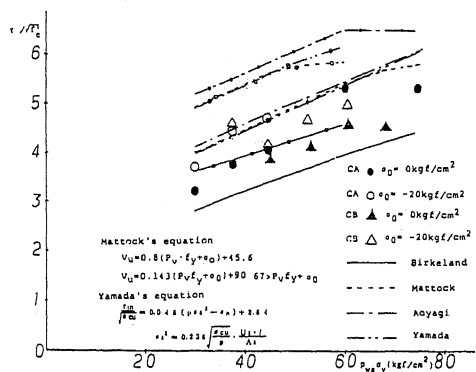|	Q(tf)	$\tau\left(\frac{kg}{cm^2}\right)$	τ/Fc	$\tau/\sqrt{Fc}$		Q(tf)	$\tau\left(\frac{kg}{cm^2}\right)$	τ/Fc	$\tau/\sqrt{Fc}$
CA1	19.2	60.0	0.17	3.24	CB1	21.7	67.8	0.23	3.91
CA2	22.2	69.3	0.20	3.75	CB2	23.0	71.9	0.24	4.15
CA3	22.5	70.3	0.21	3.80	CB3	25.5	79.8	0.27	4.60
CA4	26.8	83.4	0.24	4.61	CB4	25.6	80.0	0.27	4.62
CA5	24.0	75.0	0.22	4.07	CB5	26.0	81.2	0.26	4.69
CA6	28.0	87.5	0.26	4.74	CB6	23.3	72.8	0.23	4.20
CA7	31.6	98.7	0.29	5.35	CB7	26.0	81.2	0.26	4.69
CA8	31.5	98.4	0.29	5.34	CB8	27.8	86.9	0.28	5.02

Fig.9 Relations between Shear Strength
and Reinforcement Parameter